Experimental evaluation of linear model based control strategies for PEMFCs

R.N. Methekar , S.C. Patwardhan, R. Rengaswamy , R.D. Gudi and V. Prasad

Abstract— In this work, we investigate linear model based multivariable control schemes for proton exchange membrane fuel cells (PEMFCs). Much of the literature relies on a mechanistic model to design model predictive controllers; however, this can be a difficult and time-consuming exercise for a PEMFC. An effective approach for developing models for control purposes is to use time series analysis and develop control oriented state space models directly from input-output data. In the present work, we develop an innovation form of state space model from input-output perturbation data obtained from a PEMFC. We then demonstrate the development of infinite horizon unconstrained linear model predictive controllers (LMPC) using these models, and compare their performance to IMC based PI control. We conduct servo and regulatory control studies on an experimental single cell PEMFC system, and demonstrate that the proposed control schemes regulate the power obtained from the fuel cell as desired even in the presence of disturbances.

I. INTRODUCTION

Among fuel cells, proton exchange membrane fuel cells (PEMFCs) have evinced considerable interest because of the potential for faster start-up, higher power density, compactness, light weight and low operating temperature, and they are being considered for use in mobile and stationary applications. In terms of understanding PEMFC behavior, the development of steady state and unsteady state mechanistic models has been the focus of much of the research effort ([1],[2],[3],[4]). However, not as much attention has been paid to the control challenges arising from the complex dynamics of the PEMFC.

While fuel cells are highly nonlinear systems, most approaches described in the literature on PEMFC control are linear strategies. The two major classes of linear PEMFC controllers are those based on mechanistic models (usually linearized around a nominal operating point), and those based on black box/empirical models. Lauzze and Chmielewski [5], Choe *et al.* [6], Grujicic *et al.* [7], Pukrushpan *et al.* [8], Paradkar *et al.* [9], Bao *et al.* [10] and Zenith *et al.* [11] describe control strategies based on mechanistic models, and most of these are simulation studies. Control strategies based on empirical models are described by Methekar *et al.* [12], [14] (who use transfer functions and other empirical models, and LQG and IMC based controllers), Williams *et al.* [13] (who use models developed injecting half cosine

wave signals with PI control) and Wang *et al.* [15] (who use subspace identification and robust multivariable control).

What is missing from most previous investigations is a rigorous method to develop multivariable state space models that demonstrate fidelity to experimentally observed behavior, and to develop multivariable controllers for the PEMFC. In this work, we propose that using the *innovation form of state space models* from input-output perturbation data obtained from a PEMFC is an efficient, cost-effective approach to developing linear state space models for fuel cells. We demonstrate that these models can be used for developing infinite horizon unconstrained linear model predictive controllers (LMPC), and focus primarily on the control of power density (temperature is also controlled). Experimental verification is carried out on a single cell PEMFC set-up.

The remainder of this paper is structured as follows: model development is presented in Section II, LMPC design in Section III, and experimental results in Section IV. Finally, conclusions based on experimental results are presented in Section V.

II. IDENTIFICATION OF CONTROL-ORIENTED STATE SPACE MODELS

The mechanistic models for PEMFCs form a set of nonlinear differential algebraic equations (DAEs), represented as

$$\frac{d\mathbf{z}^{(1)}}{dt} = \mathbf{F}_1 \left[\mathbf{z}^{(1)}, \mathbf{z}^{(2)}, \mathbf{U}_T(t), \mathbf{D}(t), \mathbf{p} \right] \quad (1)$$

$$\overline{0} = \mathbf{F}_2 \left[\mathbf{z}^{(1)}, \mathbf{z}^{(2)}, \mathbf{U}_T(t), \mathbf{D}(t), \mathbf{p} \right]$$

$$\mathbf{Y}(t) = \mathbf{G} \left[\mathbf{z}^{(1)}, \mathbf{z}^{(2)} \right] + \upsilon_y(t) \quad (2)$$

where $\left[\begin{array}{cc} \mathbf{z}^{(1)T} & \mathbf{z}^{(2)T} \end{array} \right]^T \in R^n$ is the process state vector, $\mathbf{U}_T \in R^m$ the true manipulated input value, $\mathbf{D} \in \mathbf{R}^d$ the unmeasured disturbances, $\mathbf{y} \in R^r$ the vector of measured outputs corrupted with measurement noise $\upsilon_y(t)$ and $\mathbf{p} \in R^\nu$ the parameter vector. $\mathbf{U} \in R^m$ is the known (or computed) value of the manipulated inputs, and

$$\mathbf{U}_T(t) = \mathbf{U}(t) + \upsilon_u(t) \quad (3)$$

where $\upsilon_u \in R^m$ is an unknown input disturbance (assumed to be zero mean stationary), and $\mathbf{U}_T(t)$ is the true input.

In practice, the operators $\mathbf{F}_1[.], \mathbf{F}_2[.]$ and $\mathbf{G}[.]$ are seldom known exactly, and/or are too complex for controller development. Thus, the information available from the plant is the sampled sequence of input and output vectors $\Sigma_N = \{(\mathbf{Y}(k), \mathbf{U}(k)) : k = 1, 2, \dots N\}$. Given Σ_N, and defining perturbation variables $\mathbf{y}(k)$ and $\mathbf{u}(k)$ in the neighborhood of

R.N. Methekar, S.C Patwardhan and R.D. Gudi are with the Department of Chemical Engineering, Indian Insitute of Technology Bombay, India.
R. Rengaswamy is with the Department of Chemical Engineering, Texas Tech University, USA.
V. Prasad is with the Department of Chemical and Materials Engineering, University of Alberta, Canada. e-mail: vprasad@ualberta.ca

a steady state, identifying a linear time series model equates to finding a linear operator $\varphi\left[.\right]$

$$\mathbf{y}(k) = \varphi\left[\mathbf{u}(k-1), ..., \mathbf{u}(1), \mathbf{y}(k-1), ..., \mathbf{y}(1), \theta\right] + \mathbf{e}(k) \quad (4)$$

such that a suitable norm of model residuals $\{\mathbf{e}(k) : k = 1, ...N\}$ is minimized with respect to the parameter vector θ, with the effect of unmeasured disturbances being captured in the measured output sequence.

We develop an innovation form of state space model

$$\mathbf{x}(k+1) = \mathbf{\Phi}\mathbf{x}(k) + \mathbf{\Gamma}\mathbf{u}(k) + \mathbf{L}\mathbf{e}(k) \quad (5)$$
$$\mathbf{y}(k) = \mathbf{C}\mathbf{x}(k) + \mathbf{e}(k) \quad (6)$$

where $\{\mathbf{e}(k)\}$ represents a zero mean white noise sequence (covariance $\mathbf{V}$). We can directly identify matrices $(\mathbf{\Phi}, \mathbf{\Gamma}, \mathbf{L}, \mathbf{C})$ from data using the *prediction error method* (PEM) or a subspace identification method, or by canonical parameterization through transfer functions([16]): using this approach, transfer function matrices of the form

$$\mathbf{y}(k) = \mathbf{G}(q, \theta)\mathbf{u}(k) + \mathbf{H}(q, \theta)\mathbf{e}(k) \quad (7)$$

are identified and a state realization of the form (5-6) is constructed such that

$$\mathbf{G}(q) = \mathbf{C}\left[q\mathbf{I} - \mathbf{\Phi}\right]^{-1}\mathbf{\Gamma}; \ \mathbf{H}(q) = \mathbf{C}\left[q\mathbf{I} - \mathbf{\Phi}\right]^{-1}\mathbf{L} + \mathbf{I} \quad (8)$$

Here, q represents the shift operator.

For model identification, the state space model (5-6) can be cast in predictor form:

$$\mathbf{e}(k) = \mathbf{y}(k) - \mathbf{C}\widehat{\mathbf{x}}(k|k-1)$$
$$= \mathbf{y}(k) - \widehat{\mathbf{y}}(k|k-1) \quad (9)$$
$$\widehat{\mathbf{x}}(k+1|k) = \mathbf{\Phi}\widehat{\mathbf{x}}(k|k-1) + \mathbf{\Gamma}\mathbf{u}(k) + \mathbf{L}\mathbf{e}(k) \quad (10)$$

Similarly, Eq. (7) is cast into the predictor form as

$$\hat{\mathbf{y}}(k|k-1) = \mathbf{H}(q, \theta)^{-1}\mathbf{G}(q, \theta)\mathbf{u}(k) + (\mathbf{I} - \mathbf{H}(q, \theta)^{-1})\mathbf{y}(k) \quad (11)$$

The parameters $(\mathbf{\Phi}, \mathbf{\Gamma}, \mathbf{L})$ or θ are identified by minimizing a weighted 2-norm of the prediction errors:

$$\mathbf{J} = \sum_{k=1}^{N} \|\mathbf{y}(k) - \hat{\mathbf{y}}(k|k-1)\|_{W,2} \quad (12)$$

Further details of the prediction error method are found in Ljung [16] and Sodderstrom and Stoica [17]. The parameter identification procedure generates the optimal set of model parameters and an estimate of the covariance $(\mathbf{V})$ of the innovation sequence $\{\mathbf{e}(k)\}$.

There are various model forms available for such canonical parameterization. The conventional approach is to develop an ARMAX model ([16] & [17])

$$y(k) = \frac{B(q)}{A(q)}u(k) + \frac{C(q)}{A(q)}e(k) \quad (13)$$

where the coefficients of polynomials $A(q), B(q)$ and $C(q)$ are identified from data by minimizing the sum of squares of the prediction error. Alternatively, the predictor can be parameterized using orthonormal basis filters (OBF)

[18]; identification of OBF poles and the corresponding coefficients can be found in [19].

In this method, an $r \times m$ multiple input multiple output (MIMO) model is typically represented as r multiple input single output (MISO) models; these models are combined to form a realization similar to (5-6). Such models can be developed quickly by conducting experiments to excite the plant in the neighborhood of the operating point. These models capture the effects of manipulated or known inputs and unmeasured disturbances on the outputs; also, they are linear, leading to easy controller development; we choose the linear model predictive control (LMPC) approach.

III. LINEAR MODEL PREDICTIVE CONTROL (LMPC)

To develop the LMPC scheme, defining $\overline{\mathbf{x}}(k) = E\left[\mathbf{x}(k)\right]$, where $E\left[.\right]$ represents the expectation operator, we use the deterministic part of the identified state space model

$$\overline{\mathbf{x}}(k+1) = \mathbf{\Phi}\overline{\mathbf{x}}(k) + \mathbf{\Gamma}\mathbf{u}(k) \quad (14)$$
$$\overline{\mathbf{y}}(k) = \mathbf{C}\overline{\mathbf{x}}(k) \quad (15)$$

under the assumption that $E\left[\mathbf{e}(k)\right] = \overline{0}$. We assume that the model is open loop stable, and all eigenvalues of $\mathbf{\Phi}$ are strictly inside the unit circle. This model is used to generate a state estimate using an open loop observer

$$\widehat{\overline{\mathbf{x}}}(k) = \mathbf{\Phi}\widehat{\overline{\mathbf{x}}}(k-1) + \mathbf{\Gamma}\mathbf{u}(k-1) \quad (16)$$

In the LMPC formulation, given a guess of the future manipulated inputs $\{\mathbf{u}(k+j|k) : j = 0, 1, 2, ...p-1\}$, the model (14-15) is used to generate predictions over the future time window $\{k+1, k+2, .., k+p\}$ as follows

$$\widehat{\overline{\mathbf{x}}}(k+j+1|k) = \mathbf{\Phi}\widehat{\overline{\mathbf{x}}}(k+j|k) + \mathbf{\Gamma}\mathbf{u}(k+j|k) \quad (17)$$
$$\widehat{\overline{\mathbf{y}}}(k+j) = \mathbf{C}\widehat{\overline{\mathbf{x}}}(k+j|k) \quad (18)$$

for $j = 0, 1, ...p-1$ and $\widehat{\overline{\mathbf{x}}}(k|k) = \widehat{\overline{\mathbf{x}}}(k)$

where p is the prediction horizon. Model-plant mismatch is corrected for using

$$\widehat{\overline{\mathbf{y}}}_c(k+j) = \widehat{\overline{\mathbf{y}}}(k+j) + \mathbf{d}(k) \quad (19)$$
$$\mathbf{d}(k) = \mathbf{y}(k) - \mathbf{C}\widehat{\overline{\mathbf{x}}}(k) \quad (20)$$

for $j = 0, 1, ...p-1$. The degrees of freedom for shaping the future trajectory are restricted by imposing input blocking constraints

$$\mathbf{u}(k+j|k) = \mathbf{u}(k|k) \text{ for } j = 0, 1....c_1 - 1 \quad (21)$$
$$\mathbf{u}(k+j|k) = \mathbf{u}(k+c_1|k) \text{ for } j = c_1...c_2 - 1$$
$$............$$
$$\mathbf{u}(k+j|k) = \mathbf{u}(k+c_{q-1}|k) \text{ for } j = c_{q-1}...p-1$$
$$0 < c_1 < c_2 < ...c_{q-1}$$

where q is the control horizon. Given this prediction model, input constraints and the desired setpoint $\mathbf{r}(k)$, the unconstrained infinite horizon MPC problem at sampling instant k

is an optimization problem as follows

$$\begin{aligned}
\min_{\mathbf{U}_f(k)} \quad & \epsilon(k+p|k)^T \mathbf{w}_\infty \epsilon(k+p|k) \\
& + \sum_{j=1}^{p-1} \mathbf{e}_f(k+j|k)^T \mathbf{w}_E \mathbf{e}_f(k+j|k) \\
& + \sum_{j=1}^{c_{q-1}} \triangle \mathbf{u}(k+j|k)^T \mathbf{w}_{\triangle U} \mathbf{u}(k+j|k)
\end{aligned} \quad (22)$$

where

$$\mathbf{U}_f(k) = \begin{bmatrix} \mathbf{u}(k|k)^T & \mathbf{u}(k+c_1|k)^T & ... & \mathbf{u}(k+c_{q-1}|k)^T \end{bmatrix}^T$$

$$\begin{aligned}
\mathbf{e}_f(k+j|k) &= \mathbf{r}(k) - \widehat{\overline{\mathbf{y}}}(k+j|k) & (23) \\
\epsilon(k+p|k) &= \widehat{\overline{\mathbf{x}}}(k+p|k) - \overline{\mathbf{x}}_s(k) \\
\triangle \mathbf{u}(k+j|k) &= \mathbf{u}(k+j|k) - \mathbf{u}(k+j-1|k) \\
\overline{\mathbf{x}}_s(k) &= \left[\mathbf{C}(\mathbf{\Phi}-\mathbf{I})^{-1}\mathbf{\Gamma} \right]^{-1} [\mathbf{r}(k) - \mathbf{d}(k)]
\end{aligned}$$

$\mathbf{w}_E$ is a symmetric positive semidefinite error weighting matrix, and $\mathbf{w}_{\triangle U}$ is a symmetric positive definite input weighting matrix. The terminal state weighting matrix $\mathbf{w}_\infty$ is found by solving the discrete Lyapunov equation [20]

$$\mathbf{w}_\infty = \mathbf{C}^T \mathbf{w}_E \mathbf{C} + \mathbf{\Phi}^T \mathbf{w}_\infty \mathbf{\Phi} \quad (24)$$

The predicted output vector $\widehat{\mathbf{Y}}(k)$ is

$$\widehat{\mathbf{Y}}(k) = \begin{bmatrix} \widehat{\mathbf{y}}(k+1|k)^T & \widehat{\mathbf{y}}(k+2|k)^T & ..... & \widehat{\mathbf{y}}(k+p|k)^T \end{bmatrix} \quad (25)$$

We can express the prediction model as

$$\widehat{\mathbf{Y}}(k) = \mathbf{S}_x \widehat{\overline{\mathbf{x}}}(k) + \mathbf{S}_u \mathbf{U}_f(k) + \mathbf{S_I}\mathbf{d}(k) \quad (26)$$

$$\mathbf{S}_x = \begin{bmatrix} \mathbf{C}\mathbf{\Phi} \\ \mathbf{C}\mathbf{\Phi}^2 \\ ...... \\ \mathbf{C}\mathbf{\Phi}^p \end{bmatrix} \quad ; \quad \mathbf{S_I} = \begin{bmatrix} \mathbf{I} \\ \mathbf{I} \\ ...... \\ \mathbf{I} \end{bmatrix} \quad (27)$$

$$\mathbf{S}_u = \begin{bmatrix} \mathbf{C}\mathbf{\Gamma} & [\mathbf{0}] & [\mathbf{0}] & .... & [\mathbf{0}] \\ \mathbf{C}\mathbf{\Phi}\mathbf{\Gamma} & \mathbf{C}\mathbf{\Gamma} & [\mathbf{0}] & .... & [\mathbf{0}] \\ \mathbf{C}\mathbf{\Phi}^2\mathbf{\Gamma} & \mathbf{C}\mathbf{\Phi}\mathbf{\Gamma} & \mathbf{C}\mathbf{\Gamma} & ... & [\mathbf{0}] \\ ..... & ...... & .... & .... & .... \\ \mathbf{C}\mathbf{\Phi}^{p-1}\mathbf{\Gamma} & \mathbf{C}\mathbf{\Phi}^{p-2}\mathbf{\Gamma} & ... & ... & \mathbf{C}\mathbf{\Gamma} \end{bmatrix} \Xi \quad (28)$$

where Ξ is a $(p \times q)$ block matrix defined as

$$\Xi = \begin{bmatrix}
\mathbf{I}_m & [\mathbf{0}] & [\mathbf{0}] & .. & .. & [\mathbf{0}] \\
... & ... & .. & .. & .. & .. \\
\mathbf{I}_m & [\mathbf{0}] & [\mathbf{0}] & .. & .. & [\mathbf{0}] \\
[\mathbf{0}] & \mathbf{I}_m & [\mathbf{0}] & .. & .. & [\mathbf{0}] \\
... & ... & .. & .. & .. & .. \\
[\mathbf{0}] & \mathbf{I}_m & [\mathbf{0}] & .. & .. & [\mathbf{0}] \\
... & ... & .. & .. & .. & .. \\
[\mathbf{0}] & ... & .. & .. & [\mathbf{0}] & \mathbf{I}_m \\
... & ... & .. & .. & .. & .. \\
[\mathbf{0}] & ... & .. & .. & [\mathbf{0}] & \mathbf{I}_m
\end{bmatrix} \quad (29)$$

$\mathbf{I}_m$ is an identity matrix of dimension m and $[\mathbf{0}]$ an $(m \times m)$ null matrix. $\mathbf{S}_u$ is the system's dynamic matrix. The future prediction error vector $\mathbf{E}(k)$ is

$$\mathbf{E}(k) = \mathbf{S_I}\mathbf{r}(k) - \widehat{\mathbf{Y}}(k) \quad (30)$$

The unconstrained version of LPMC can be re-cast as

$$\min_{\mathbf{U}_f(k)} \frac{1}{2}\mathbf{U}_f(k)^T \mathbf{H}\mathbf{U}_f(k) + \mathbf{U}_f(k)^T F(k) \quad (31)$$

where

$$\mathbf{H} = 2(\mathbf{S}_u^T \mathbf{W}_E \mathbf{S}_u + \mathbf{\Lambda}^T \mathbf{W}_U \mathbf{\Lambda} + \mathbf{\Omega}^T \mathbf{W}_\infty \mathbf{\Omega})$$

$$F(k) = -2 \begin{bmatrix} (\mathbf{S_I}\mathbf{r}(k) - \mathbf{S}_x\widehat{\mathbf{x}}(k|k-1) - \mathbf{S}_d\mathbf{d}(k|k))^T \\ \mathbf{W}_E\mathbf{S}_u \\ + (\mathbf{\Lambda}_0\mathbf{u}_{k-1})^T \mathbf{W}_U\mathbf{\Lambda} \\ +(\mathbf{\Phi}^p\widehat{\mathbf{x}}(k|k-1) - \hat{\mathbf{x}}_s(k))\mathbf{W}_\infty\mathbf{\Omega} \end{bmatrix}$$

$$\mathbf{\Omega} = \begin{bmatrix} \mathbf{\Phi}^{p-1}\mathbf{\Gamma} & \mathbf{\Phi}^{p-2}\mathbf{\Gamma} & ... & ... & \mathbf{\Gamma} \end{bmatrix}$$

$$\begin{aligned}
\mathbf{W}_E &= block\ diag \begin{bmatrix} \mathbf{w}_e & \mathbf{w}_e & .... & \mathbf{w}_e \end{bmatrix} & (32) \\
\mathbf{W}_U &= block\ diag \begin{bmatrix} \mathbf{w}_u & \mathbf{w}_u & .... & \mathbf{w}_u \end{bmatrix}
\end{aligned}$$

$$\Delta\mathbf{U}_f(k) = \mathbf{\Lambda}\,\mathbf{U}_f(k) - \mathbf{\Lambda}_0\mathbf{u}(k-1) \quad (33)$$

$$\mathbf{\Lambda} = \begin{bmatrix} \mathbf{I} & [\mathbf{0}] & [\mathbf{0}] & [\mathbf{0}] \\ -\mathbf{I} & \mathbf{I} & [\mathbf{0}] & [\mathbf{0}] \\ ... & ... & ... & ... \\ [\mathbf{0}] & .... & -\mathbf{I} & \mathbf{I} \end{bmatrix} \quad ; \quad \mathbf{\Lambda}_0 = \begin{bmatrix} \mathbf{I} \\ [\mathbf{0}] \\ ... \\ [\mathbf{0}] \end{bmatrix} \quad (34)$$

This unconstrained problem can be solved analytically to compute a closed form control law

$$\mathbf{u}(k) = \mathbf{\Lambda}_0^T \mathbf{H}^{-1}F(k) \quad (35)$$

IV. EXPERIMENTAL EVALUATION

The efficacy of the proposed model based control schemes was evaluated using a single cell PEMFC set-up at the Department of Chemical Engineering, Clarkson University, USA. The performance of the LMPC is compared with IMC based PI controllers (designed as in [21]). The SISO case with power output controlled by manipulating hydrogen flowrate is considered. Nominal operating conditions are listed in Table I. The closed loop performance is assessed using the following performance indices:

- **Integral Square Error (ISE)**: For the ith output, this index is defined as

$$(ISE)_i = \sum_{k=1}^{N_s} [\mathbf{r}_i(k) - \mathbf{y}_i(k)]^2$$

- **Integral Control Effort (ICE)**: For the ith input, this index is defined as

$$(ICE)_i = \sum_{k=1}^{N_s} [\mathbf{u}_i(k) - \mathbf{u}_i(k-1)]^2$$

- **Settling time:** Defined as the time the output requires to reach $\pm 5\%$ of the final value after a step change in setpoint.

TABLE I

NOMINAL OPERATING CONDITIONS FOR EXPERIMENTAL STUDY

Parameter	Expt. Value	Sim. Value
Inlet flow rate of hydrogen	70 (sccm)	1.75×10^{-5} (mol/sec)
Inlet flow rate of oxygen	100 (sccm)	7.6×10^{-4} (mol/sec)
Cell Temperature (^{0}C)	70	80
Anode Inlet Temperature (^{0}C)	70	80
Cathode Inlet Temperature(^{0}C)	70	80
Back pressure at anode (psi)	0	NA
Back pressure at cathode (psi)	0	NA
Cell voltage (V)	0.6	0.53

A. Single Cell PEMFC Set-up

The single cell PEMFC used is a commercially available fuel cell from Fuel Cell Technologies, Inc. The experimental set-up consists of a humidifier, fuel cell and an electronic load. The membrane electrode assembly (MEA) is a high performance membrane from PEAMEAS (E-TEK), Inc., with an active area of 10 cm^2. The whole assembly (MEA, gaskets, flow channels) is supported by stainless steel plates on both sides. The electron collector plates are placed between the gas flow channel and supporting plates. The hydrogen and oxygen flows are passed through external humidifiers (make: ElectroChem, Inc.) before being injected into the fuel cell. Separate mass flow controllers (make: ElectroChem Inc., range: $0-200$ sccm, back-pressure adjustment: $0-60$ psi) are used for manipulating hydrogen and oxygen flow rate to the PEMFC. The fuel cell is connected to a variable electronic load (Agilent N 3300A DC electronic load) operated under constant voltage mode. The fuel cell temperature is kept constant using a separate electronic controller. The system is connected to a PC using a data acquisition system (make: Measurement Computing Corp.) through the USB port. A schematic diagram of the entire set-up is shown in Figure [1].
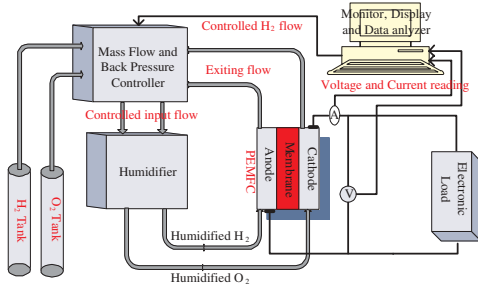

Fig. 1. Schematic diagram of experimental set-up

B. Model Identification

Figure [2] shows the nominal steady state relationship between the power output and inlet hydrogen flow rate generated through a series of steady state experiments. The sensitivity of power output with respect to the H$_2$ flow-rate is almost constant until 90 sccm, and it practically reduces to zero above 100 sccm. On the other hand, at very low hydrogen flow rate in the channels, starvation of the reactant is a real possibility. Hence, we select set points in the range

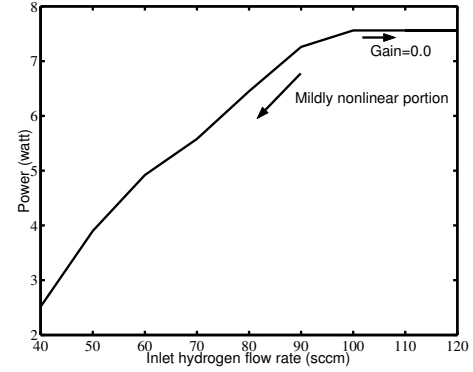$4.5 - 6$ W. A control relevant state space model is identified

Fig. 2. Steady state input-output relationship (hydrogen flow rate - power)

by perturbing the inlet hydrogen flow rate using multilevel random signals with standard deviations of $\sigma_{u1E} = 7.38$ sccm with switching time 10 sec. After collecting the input-output data, the data set is divided into an identification data set and a validation data set. The identification data set contained 1500 data samples, whereas the validation data set contained 500 data samples. We first obtain an ARMAX model of the form

$$y(k) = \frac{b_1 q^{-1} + b_2 q^{-2}}{1 + a_1 q^{-1} + a_2 q^{-2}} u(k) + \frac{1 + c_1 q^{-1} + c_2 q^{-2}}{1 + a_1 q^{-1} + a_2 q^{-2}} e(k)$$

and then convert it into a state space model as follows

$$\mathbf{\Phi} = \begin{bmatrix} -a_1 & 1 \\ -a_2 & 0 \end{bmatrix} ; \quad \mathbf{\Gamma} = \begin{bmatrix} b_1 \\ b_2 \end{bmatrix} ;$$

$$\mathbf{L} = \begin{bmatrix} c_1 - a_1 \\ c_2 - a_2 \end{bmatrix} \quad C = \begin{bmatrix} 1 & 0 \end{bmatrix}$$

The identified model parameters are $a_1 = 1.7559$, $a_2 = 0.7659$; $b_1 = 8.5033 \times 10^{-6}$; $b_2 = 8.1133 \times 10^{-4}$; $c_1 = 1$; $c_2 = 0$ and the covariance of the innovation sequence $\{e(k)\}$ is 0.0424. To validate the identified model, we have
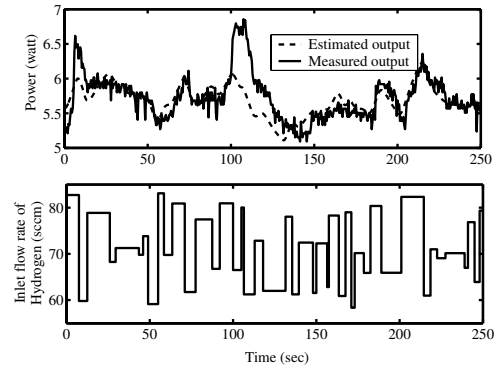

Fig. 3. Validation of identified model

compared the simulated transient behavior of the identified model (given by equations 14-15 with $\widehat{\mathbf{x}}(0) = \overline{0}$) with the experimental data(Figure [3]). The identified model predicts the transient behavior reasonably well. While the model is identified and tested in a relatively small region of operation,
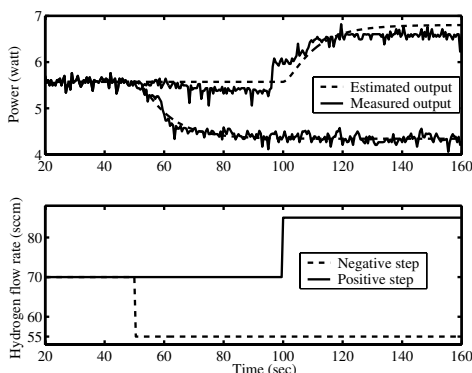
Fig. 4. Step response validation of identified model

Fig. 5. IMC based PI controller performance on experimental set-up

Fig. 6. LMPC controller perfromance on experimental set-up

re-identification (if required) in other regions of the operating space should only take a few seconds of experimentation.

We have also validated the model by comparing step responses of the process with the model. Step changes were introduced in both directions, i.e., positive and negative steps; these are shown in Figure [4] along with the model predictions. The process has mildly nonlinear behavior in this range, and the steady state sensitivity in positive and negative directions are different. The linear model identified from data generated using perturbations on either side of the steady state, however, generates a symmetric response using an average steady state gain.

C. Controller Performance

The LPMC and IMC based PI controllers are evaluated for servo and regulatory problems. The weighting matrices used in LPMC are $\mathbf{w}_E = 1$; $\mathbf{w}_{\Delta U} = 0$; $\mathbf{w}_\infty = 0$. The prediction horizon and control horizon for LPMC are $p = 70$ and $q = 1$, respectively. The IMC tuning parameters for the PI controller are $k_c = 8.71/\lambda, \tau_i = 5$ sec. $\lambda (= \tau/3)$ is the desired close loop time constant. τ is the open loop time constant of the system (5 sec). To make our conclusions independent of any specific experimental runs, we carried out seven experiments with each control strategy, and the performance comparison is based on average values over these experiments.

In the servo control problem, the controllers are expected to track a sequence of two setpoint changes (6 watt and 4.5 watt), and the typical performance is shown in Figures (5) and (6). Performance indices averaged over 7 runs are presented in Table II. LPMC performs better than IMC based PI in terms of ISE, but requires a slightly higher settling time. The control effort for LMPC is slightly smaller than that of IMC based PI, which might be beneficial in terms of fuel efficiency.

The response of control strategies for positive and negative changes in set point is slightly different, because the model fits better in the negative direction. In the positive direction, all controllers take slightly more time to track the set point. This can easily be corrected using a gain-scheduled approach. In the positive direction, we observe a large number of sudden jumps; this is probably due to
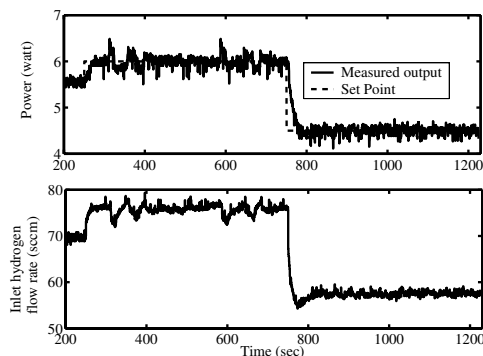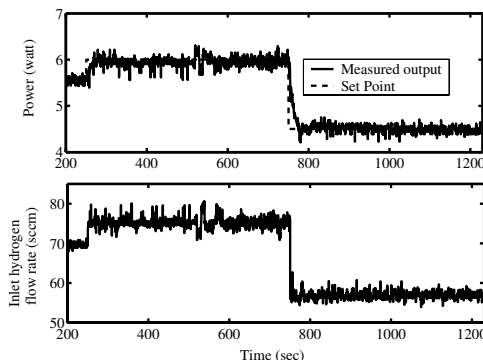
flooding at the cathode. As a large amount of current is withdrawn from the PEMFC, the reaction rate is high, which produces more water and may cause flooding.

Figures [7 & 8] present the regulatory performance of the control schemes in response to a 0.05V step disturbance in the cell voltage. An increase in voltage should decrease the current, which should cause the inlet flow rate of hydrogen to increase to maintain the same power requirement. However, we observed a decrease in the inlet flow rate of hydrogen. This is probably due to an increase in the utilization factor, because there is more current produced. This, in turn, results in a decrease in effluent coming out of the fuel cell channel, which decreases the amount of water coming out from fuel cell, which increases membrane humidity, and results in an overall increase in current. Hence, there is a decrease in the hydrogen flow rate requirement. The performance indices for regulatory control are presented in Table III.

TABLE II

CONTROLLER PERFOMANCE INDICES FOR SET POINT TRACKING

	ISE	ICE	Settling time (sec)
	$Mean$ $(Std.dev.)$	$Mean$ $(Std.dev.)$	$Mean$ $(Std.dev.)$
IMC based PI	32.06 (1.34)	9.02×10^6 (4.16×10^4)	39.0 (6.54)
LMPC	27.88 (4.47)	8.97×10^6 (7.54×10^4)	40.0 (10.37)

TABLE III

CONTROLLER PERFOMANCE INDICES FOR REGULATORY CONTROL

(DISTURBANCE REJECTION)

Power	ISE	ICE	Settling time (sec)
IMC based PI	4.37	1.53×10^6	40
LMPC	4.36	1.55×10^6	40

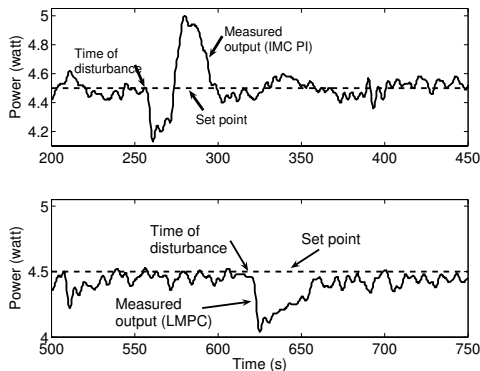Both controllers have practically identical performance for disturbance rejection.

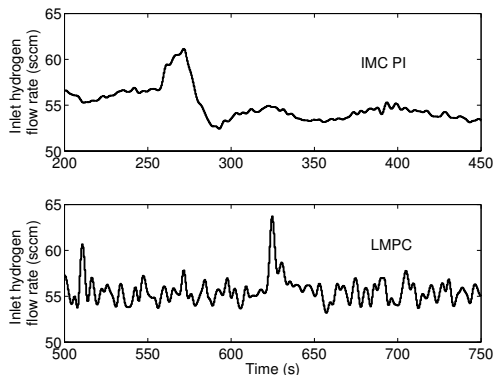Fig. 7.   Controller performance in regulatory control (disturbance rejection)

Fig. 8.   Manipulated variable action in regulatory control (disturbance rejection)

V. CONCLUSIONS

Model based multivariable control schemes such as MPC can be used to control a PEMPC system effectively. A cost effective approach is to develop models using time series analysis directly from input-output data. Identification of the models requires minimal experimentation, with excitation provided using multilevel random signals. We develop the innovation form of state space models directly from input-output data obtained by conducting perturbation studies on PEMFCs and show how these models can be used to develop an infinite horizon unconstrained linear model predictive controller (LMPC). Experimental verification was conducted on a single cell PEMFC set-up. While the LMPC provides

satisfactory performance for servo and regulatory control of fuel cell power, IMC based PI control provides comparable performance. The real utility of the LMPC is in multivariable control (controlling power and temperature, for example) and the inclusion of constraints (related to flooding, for example), and in operating at the optimum efficiency conditions; our current and future research focuses on these aspects.

REFERENCES

[1] D. M. Bernardi, M. W. Verbrugge, A mathematical model of the solid-polymer-electrolyte-fuel cell, J. Elctrochem. Soc., 139 (9) (1992) 2477-2491.
[2] P. R. Pathapati, X. Xue, J. Tang, A new dynamic model for predicting transient phenomena in a PEM fuel cell system, Renewable Energy, 30 (2005) 1-22.
[3] J. Golbert, D. Lewin, Model-based control of fuel cells: (1) Regulatory control, J. Power Sources, 135 (2004) 135-151.
[4] M. Rao, R. Rengaswamy, Dynamic characteristics of spherical agglomerate for study of cathode catalyst layer in proton exchange membrane fuel cells, J. Power Sources, 158 (2006) 110-123.
[5] K. C. Lauzze, D. J. Chmielewski, Power control of a polymer electrolyte membrane fuel cell, Ind. Eng. Chem. Res., 45 (2006) 4661-4670.
[6] S. Y. Choe, J. G. Lee, J. W. Ahn, S. H. Baek, Integrated modeling and control of a PEM fuel cell power system with a PWM DC/DC converter, J. Power Sources, 164 (2007) 614-623.
[7] M. Grujicic, K. M. Chittajallu, E. H. Law, J. T. Pukrushpan, Model-based control strategies in the dynamic interaction of air and fuel cell, J. Power and Energy, 218A (2004) 487-499.
[8] J. T. Pukrushpan, A. G. Stefanopolou, H. Peng, Modeling and control of PEM fuel cell stack system, Proc. American Control Conference, (2002) 3117-3122.
[9] A. Paradhkar, A. Davari, A. Feliachi, T. Biswas, Integration of a fuel cell into the power system using an optimal controller based on disturbance accommodation control theory, J. Power Sources, 128 (2004) 218-230.
[10] C. Bao, M. Ouyang, B. Yi, Modeling and control of air stream and hydrogen flow with recirculation in a PEM fuel cell system -II linear and adaptive nonlinear control, Int. J. Hydrogen Energy, 31 (2006) 1897-1913.
[11] F. Zenith, S. Skogestad, Control of fuel cell power output, J. Process control, 17 (2007) 333-347.
[12] R. N. Methekar, V. Prasad, R. D. Gudi, Dynamic analysis and linear control strategies for proton exchange membrane fuel cell using a distributed parameter model, J. Power Sources, 165 (2007) 152-170.
[13] K. A. Williams, W. T. Keith, M. J. Marcel, T. A. Haskew, W. S. Shepard, B. A. Todd, Experimental investigation of fuel cell dynamic response and control, J. Power Sources, 163 (2007) 971-985.
[14] R. N. Methekar, V. Prasad, S. C. Patwardhan, R. D. Gudi, Control of PEMFC using empirical dynamic models in an IMC and LQG framework, AIChE Annual meeting, Salt lake city, Utah, USA, (2007).
[15] F. C. Wang, H. T. Chen, Y. P. Yang, J. Y. Yen, Multivariable robust control of a proton exchange membrane fuel cell, J. Power Sources, 177 (2) (2008) 393- 403.
[16] L. Ljung, Syetem Identification: Theory for the user, Second edition, Prentice Hall Inc., Eaglewood Cliffs, New Jersy.
[17] T. Soderstorm, P. Stoica, System Identification, Prentice Hall Inc.,Upper Saddle River, NJ, USA.
[18] P. Heuberger, P. Van Den Hof, B. Wahlberg, Modeling and identification with rotational orthogonal basis functions, Springer Verlag, London, 2005.
[19] S. C. Patwardhan, S. L. Shah, From data to diagnosis and control using generalized orthonormal basis filter. Part I: Development of state observers, J. Process Control, 15 (7) (2005) 819-835.
[20] R. Muske, J. B. Rawlings, Model predictive control with linear models, AIChE J., 39 (1993), 262-287.
[21] B. W. Bequette, Process control: modeling, design and simulation, Prentice-Hall, Inc 2003.